INQUA Focus Group Earthquake Geology and Seismic Hazards

paleoseismicity.org

Paleoseismology of the Western Garlock Fault at Campo Teresa, Tejon Ranch, Southern California

Gath, Eldon (1) and Rockwell, Thomas (2)

(1) Earth Consultants International, Santa Ana, California, USA. gath@earthconsultants.com.
(2) San Diego State University, San Diego, California, USA.

***Abstract**: The 250-km-long northeast-trending Garlock fault in southern California bounds extension on the north from right-laterally slipping blocks to the south. Multiple paleoseismic sites have been published for the central and eastern segments of the fault, but only Twin Lakes on the western segment. A geotechnical investigation at Campo Teresa, 25 km west of Twin Lakes generated data for the timing of the last 2-4 rupture events. Two trenches exposed the northern and southern fault traces within a narrow stepover. The exposures allowed us to constrain displacements and ages based on two radiocarbon dates from colluvial deposits; two events since 1710±40 ybp and likely two events 1710 - 4100±40 ybp. The MRE and penultimate events appear to be similar 4-m left-lateral events on the southern fault, each with about 2 m of vertical separation on the northern fault.*

***Key words**: Tectonic geomorphology, Paleoseismology, Garlock fault*

INTRODUCTION

The 250-km Garlock fault, one of the principal active faults in southern California, separates the Basin-and-Range extensional terrane to the north from the Mojave strike-slip faulting (Eastern California Shear Zone) to the south (Fig. 1). The fault appears to have initiated movement about 9 to 10 million years ago (Carter, 1987, Loomis and Burbank, 1988) and has since accumulated 56±8 km of sinistral displacement (Smith, 1962; Davis and Burchfield, 1973), providing a Miocene to present average slip rate of 5-7 mm/yr.

McGill and Sieh (1991) divide the Garlock fault into western, central and eastern segments. The western segment extends 100 km from the fault's intersection with the San Andreas fault near Frazier Park, eastward to the 3.5 km-wide Koehn Lake stepover. The central segment extends from Koehn Lake 105 km eastward to near Quail Mountain (Fig. 2), where the fault makes a distinct 15° bend. The eastern segment extends to the southern end of Death Valley.

Evidence for late Quaternary and Holocene activity is abundant along the length of the fault. Offset and deflected streams, offset alluvial fans, scarps, sag ponds, and linear valleys are well documented (Clark, 1973). Several studies have determined Holocene slip rates and event chronologies across the three segments (Fig. 2). At Searles Lake, McGill and Sieh (1993) determined a Holocene slip rate of 4-9 mm/yr, with a best estimate of 5-7 mm/yr, which is consistent with a rate of 5.3 +1/-2 by Ganev et al. (2012). These late Pleistocene-Holocene rates are similar to the Miocene-to-present rate, although almost double the current geodetic rate, leading to speculation that there are discrete cycles of strain along the Garlock fault (Dolan et al., 2016).

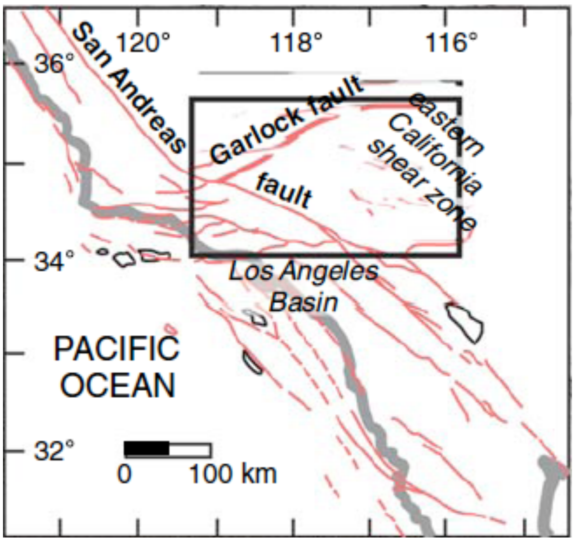

Figure 1: Location of the Garlock fault in southern California. Inset box represents the area shown in Fig. 2

The slip rate of the western segment is constrained between 5.3-10.7 mm/yr (McGill et al., 2009). Considering the continuity of the fault and the absence of major structures that could decrease the average rate determined for the central section of the fault, this rate is unlikely to be correct.

Historically, the Garlock fault has been characterized by low levels of background seismicity, and the fault has not produced any large earthquakes with surface rupture, but the historical record in this area only goes back to the early to mid 1800s. Tectonic, geomorphic and paleoseismic investigations, in contrast, demonstrate that the Garlock has repeatedly failed in large surface-rupturing earthquakes throughout the Holocene (Burke, 1979; McGill and Sieh, 1991, 1993; McGill et al., 2009;

Gath, E. and T. Rockwell, 2018, Paleoseismology of the Western Garlock Fault at Campo Teresa, Tejon Ranch, Southern California; in 9th International INQUA Meeting on Paleoseismology, Active Tectonics and Archeoseismology (PATA), 25 – 27 June 2018, Possidi, Greece, p. 71-74.

LaViolette et al., 1980; McGill and Rockwell, 1998; Dawson et al., 2003, Madugo et al., 2012).

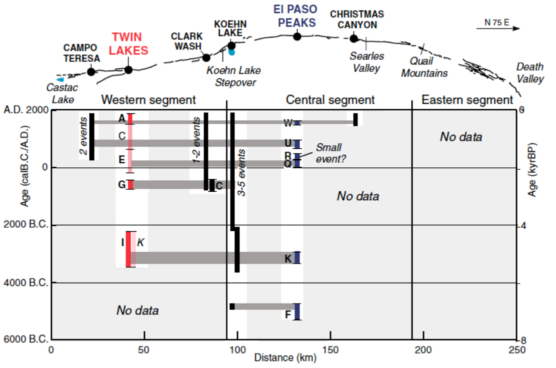

Figure 2: Earthquake chronologic correlations along the Garlock fault (Madugo et al., 2012). The Campo Teresa site is the westernmost paleoseismic site.

McGill and Sieh (1991), using offset gullies, terrace risers, channel walls, shutter ridges and other geomorphic features, determined that the central Garlock fault typically fails in large earthquakes with 3-7 m of slip. The past three earthquakes on the central segment near El Paso Peaks, all of which occurred in the past 1800 years, appear to have produced 18 m of slip (McGill and Rockwell, 1998; McGill and Sieh, 1991). Deeper trenching at the same site (Dawson et al., 2003) showed that six large earthquakes occurred during the past 7000 years along the central Garlock fault, with four of them during the past 2000 years. From this, they speculated that strain release was not cyclic, but rather occurred in clusters that may correlate to seismic activity in the Eastern California Shear Zone (Rockwell et al., 2001; Dolan et al., 2016). This is consistent with earlier work by Burke (1979) that demonstrated 9-17 events during the past 15,000 years near Koehn Lake, yielding a longer-term average recurrence rate of 860-1600 years.

Along the western segment, Stepp et al. (1980) found evidence for two Holocene surface ruptures at the Twin Lakes site, with the most recent occurring less than 890 ± 195 radiocarbon years BP. Later at Twin Lakes, Madugo et al. (2012) interpreted up to six events in the last ~5600 years through the site, including new timing constraints on the past two events (Fig. 2). McGill and Sieh (1991) identified geomorphic evidence for large slip events, with up to 7 m of displacement per event west of Koehn Lake. These observations suggest that the western Garlock fails about as frequently as the central Garlock, and may even fail together in very large earthquakes, as initially suggested by McGill and Sieh (1991). Fig. 2 illustrates the earthquake chronologies at each of the paleoseismic sites along the Garlock fault, and suggests that many of them can be correlated across multiple sites. The Campo Teresa site is the westernmost site with event data that have been used for event correlations. These data were generated during a geotechnical fault hazard study for planning of the Tejon Ranch (Fig. 3), and details of the event evidence at the site have never before been published. This paper provides the documentation for that site.

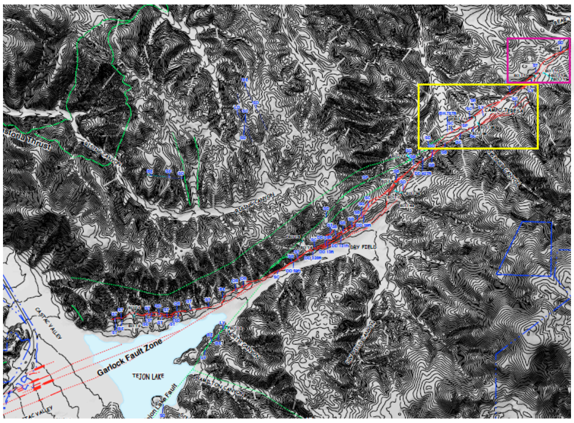

Figure 3: Geomorphic mapping of the Garlock fault along the extreme western segment across Tejon Ranch. Rattlesnake Canyon (Fig. 4) is shown by the pink box and the Campo Teresa site (Fig. 5) by the yellow box.

FAULT MORPHOLOGY ON TEJON RANCH

Across Tejon Ranch, the Garlock fault has tectonic geomorphology similar to the more easterly sections of the fault. The fault is readily expressed across the landscape by left-laterally deflected drainages, shutter ridges, and side-hill benches (Fig. 4).

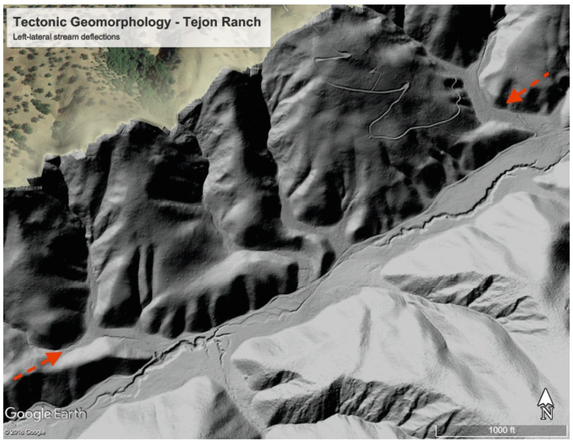

Figure 4: Tectonic geomorphology along Rattlesnake Canyon on Tejon Ranch, about 1 km NE of the Campo Teresa trenching site. The main Garlock fault trace is shown by the red arrows. The canyons are all left-laterally deflected about 125 m.

TRENCHING RESULTS

The Garlock fault is well expressed in the Campo Teresa area. Trenches T-9a and T-9b were located on the southern part of a linear valley, Trench T-10 was extended across a linear fault scarp on the north side of the valley (Fig. 5). Trenches T-9a and T-10 (Fig. 5) exposed fault strands that bound both sides of the linear valley. Below we discuss the findings in trench T-10 followed by T-9a and b.

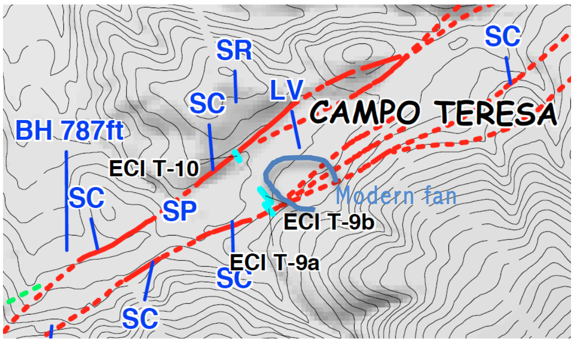

Figure 5: Campo Teresa trenching site showing the geomorphic mapping (SC-scarp, SR-sidehill ridge, SP-spring, LV-linear valley, BH-beheaded drainage) and the sites for trenches 9a&b and 10. Modern fan margin shown by blue line; with channel along western margin offset ~8 m through trench 9a.

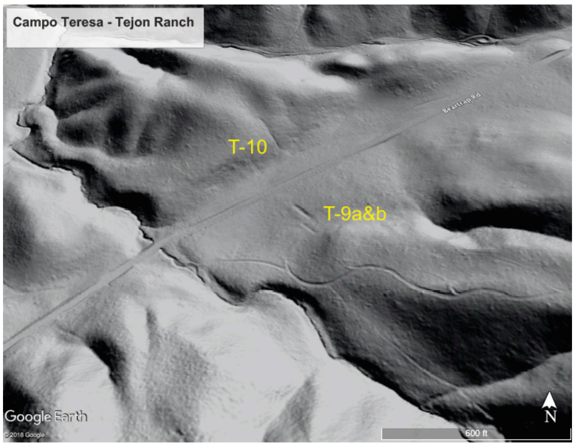

Figure 6: LiDAR image of the Campo Teresa area of Fig. 5 with the trench depressions still visible. Note the left-lateral stream deflection to the left of the T-9 trenches, but the lack of a similar deflection across the lineament trenched by T-10.

Trench T-10 was placed across a linear scarp on the north side of the Campo Teresa valley. The excavation was 24 m long and up to 4 m deep. Limestone bedrock forms the hillside in the northern portion of the trench with colluvium and alluvium present in the central and southern portions, respectively (Fig. 7). The colluvium in this trench consists of friable, massive silty sand with scattered pebbles but no large limestone clasts. The limestone in this area is highly fractured and locally sheared within the fault zone.

Two primary fault traces, about a meter apart, trending northeast and dipping to the south were observed within the bedrock. Both faults deform the overlying colluvium, and both vertically deform the base of the modern topsoil horizon similar amounts. A piece of detrital charcoal from the faulted colluvium yielded a radiocarbon age of 1710± 40 BP (Fig. 7). Based on its stratigraphic position immediately beneath a buried, weakly developed paleosol (buried A horizon), we interpret that this sample has experienced two rupture events, as follows. The penultimate event occurred when the paleosol was at the ground surface, down-dropping it at least 1 m vertically against the limestone and rotating it to subhorizontal.

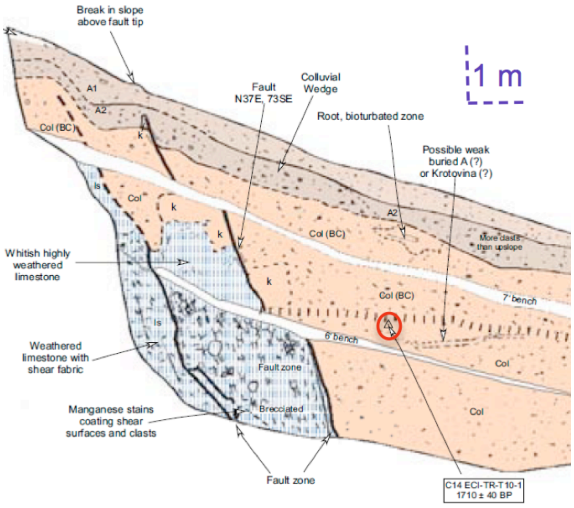

Figure 7: Graphic log of east wall of Trench T-10. Limestone is in blue, colluvium in orange, and colluvium-derived modern A-soil horizon, in brown. Red circle indicates the location of the 1710 ybp radiocarbon date from within the colluvium.

The paleosol and scarp were subsequently buried by 2 m of colluvial sediments reestablishing the slope. The most recent event generated an additional 0.7-1 m of vertical separation on the same southernmost fault, with the formation of a minimum of a 0.5-0.7m surface scarp on both faults. The total vertical rupture separation, summed across the fault zone, is ~2 m in the penultimate event and ~1.5-2 m in the MRE. Lateral slip, if any, cannot be determined from this exposure.

Trench T-9a was located at the gentle break in slope along the southern margin of the valley and was approximately 30 m long by 3 m deep (Fig. 6). The geologic units exposed in this trench included a surficial layer of colluvium underlain by granitic bedrock in the southeast (up-slope) portion of the trench and younger alluvium at the northwest end of the trench (Fig. 7). The bedrock is composed of friable, highly weathered Tejon Lookout granite. The colluvium consists of friable pebbly silty sand with weak soil development and a notable absence of granitic clasts.

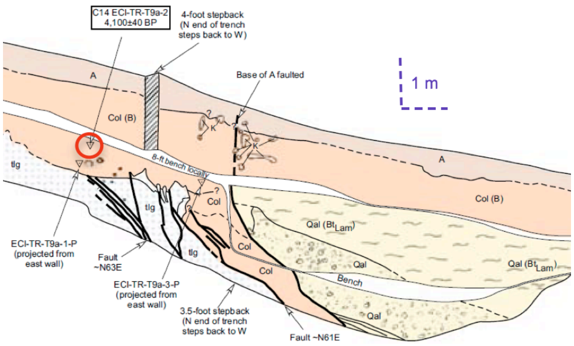

Figure 8: Graphic log of west wall of Trench 9a. Granite in white, colluvium in orange, alluvium in yellow, and modern colluvium-derived A soil horizon in brown. Red circle indicates the location of the 4100 ybp radiocarbon date from within the older colluvium, capped by younger colluvium above the bench.

A piece of detrital charcoal within the colluvium yielded a radiocarbon age of 4,100 ± 40 BP. This colluvium overlies several prominent faults within the bedrock as well as a fault that juxtaposes bedrock and older colluvial wedges faulted between the bedrock and the alluvial channel (Fig. 8). The alluvium is comprised of weakly stratified pebbly sand atop a clast-supported pebble gravel derived from an alluvial fan to the east (Fig. 5). Soil formation within the sandy alluvium is limited to argillic (Bt) lamellae. The dated colluvium is overlain by another colluvial deposit, correlated to the 1710 ybp unit in T-10, that also overlies the alluvial deposits. The northernmost fault truncates the older colluvium against the alluvial units, continues through the overlying colluvium, and displaces the base of the A soil developed on the youngest colluvial deposit (Fig. 8). We interpret the truncation of the 4300 ybp colluvium as representing an earlier event pre-1710 ybp, and the offset, but undated, colluvial wedges within the fault zone suggest the possibility of more than one event in the time interval between 4300 and 1710 ybp.

The faults trend ~N62E and dip variably to the north. The fault exposed in Trench T-9a has a dominant lateral component and is along strike with the strand that beheads and left-laterally deflects a third-order drainage ~240 m (BH 787 ft on Fig. 5). Based upon field measurements of the fan margins, the fault has translated the alluvial fan deposits exposed in the trench (Fig. 8) a minimum of 8 m left-laterally, and up to 1 m vertically (Fig. 5). This alluvial channel deposit is stratigraphically equivalent to the paleosol in T-10 (Fig. 7) implying it is also about 1710 ybp and would have experienced two displacement events [see discussion of T-10].

Trench T-9b was located north of Trench T-9a to look for additional faults basinward (Figs 5 & 6). The trench measured approximately 38 m long by 4.5 m deep and exposed younger alluvium consisting of crudely bedded, friable, silty pebbly sand and sandy gravel with weak soil development similar in age to the uppermost soils in T-9a. No faults or fractures were observed within this trench indicating that the principal faults are on the margins of the valley.

CONCLUSIONS

The Campo Teresa site provides documentation for at least two western Garlock fault ruptures within the past 1700 years, and at least one additional event (likely two) between 1700 and 4100 ybp. The MRE is expressed by the 1.5-2 m vertical displacement of the modern surface soils overlying buried colluvial and alluvial units in T-10 (Fig. 8). Those colluvial deposits, and capping weak soil, were previously down-dropped a similar 2 m post-1700 ybp (Fig. 8). The 4100 ybp colluvial unit overlies several fault traces, but is truncated by a fault that pre-dates the penultimate event of about 1700 ybp (Fig. 7). The younger alluvial fan deposits exposed in T-9a were left-laterally offset about 8 m in 2 events. Those same two events likely generated the 2-m/event vertical separations in T-10. The two post-1710 ybp events were used by Madugo et al. (2012) in the along-fault event correlation (Fig. 2). Given that the data support the occurrence of at least one and probably two or more events between 1710 and 4100 ybp, these events may well correlate with the third and fourth events at the Twin Lakes site (Fig. 2).

Acknowledgements: This work was undertaken by Earth Consultants International as part of a multi-year geologic hazards investigation of Tejon Ranch for planning of their Mountain Village development project. The entire report can be accessed at http://www.co.kern.ca.us/planning/pdfs/eirs/TMV/TejonMountainVillage_App_G1.pdf. The trenches were logged by Aaron Meltzner, Chris Walls, Altangerel Orgil, and Molly Zorba. Tania Gonzalez and Chris Madugo provided valuable review of the paper.

REFERENCES

Burke, D.B., 1979, Log of a trench in the Garlock fault zone, Fremont Valley, California, U.S. Geol. Survey Misc. Field Studies Map MF-1028.

Clark, M. M., 1973, Map showing recently active breaks along the Garlock and associated faults, California, U.S. Geol. Survey Map I-741.

Dawson, T. E., S.F. McGill, and T.K. Rockwell, 2003, Irregular recurrence of paleoearthquakes along the central Garlock, near El Paso Peaks, California, J. Geoph. Res. 108, 2356–2385.

Dolan, J.F., L.J. McAuliffe, E.J. Rhodes, S.F. McGill, R. Zinke, 2016, Extreme multi-millennial slip rate variations on the Garlock fault, California: Strain super-cycles, potentially time-variable fault strength, and implications for system-level earthquake occurrence, Earth and Planetary Sci. Letters 446, 123–136.

Ganev, P.N., J.F. Dolan, S.F. McGill, and K.L. Frankel, 2012, Constancy of geologic slip rate along the central Garlock fault: Implications for strain accumulation and release in southern California, Geophysical J. Int. 190, no. 2, 745–760.

LaViolette, J.W., G.E. Christenson, and J.C. Stepp, 1980, Quaternary displacement on the western Garlock fault, southern California, in Geology and Mineral Wealth of the California Desert, Santa Ana, California, D.L. Fife and A.R. Brown (Editors), South Coast Geol. Soc., 449–456.

Madugo, C.M., J.F. Dolan, and R.D. Hartleb, 2012, New Paleoearthquake ages from the Western Garlock Fault: Implications for regional earthquake occurrence in Southern California, B. Seism. Soc. of America, V. 102, N. 6, 2282–2299.

McGill, S.F., and T.K. Rockwell, 1998, Ages of late Holocene earthquakes on the central Garlock fault near El Paso Peaks, California, J. Geophysical Res. 103, no. B4, 7265–7279.

McGill, S.F., and K. Sieh, 1991, Surficial offsets on the central and eastern Garlock fault associated with prehistoric earthquakes, J. Geophysical Res. 96, 21,597–21,621.

McGill, S.F., and K. Sieh, 1993, Holocene slip rate of the central Garlock fault in southeastern Searles valley, California, J. Geophysical Res. 98, 14,217–14,231.

McGill, S.F., S.G. Wells, S.K. Fortner, H.A. Kuzma, and J.D. McGill, 2009, Slip rate of the western Garlock fault, at Clark Wash, near Lone Tree Canyon, Mojave Desert, California, Geol. Soc. Am. Bull. 121, 536–554, doi: 10.1130/B26123.1.

Stepp, J.C., J.W. LaViolette, and G.E. Christenson, 1980, Seismic hazard of the western portion of the Garlock fault, U.S. Geol. Survey, Open-File Rep., OF 80-1172.